International Journal of Pharmaceutics 457 (2013) 214–223

Contents lists available at ScienceDirect

International Journal of Pharmaceutics

journal homepage: www.elsevier.com/locate/ijpharm

Skin electroporation for transdermal drug delivery: The influence of the order of different square wave electric pulses

Barbara Zorec[a,1], Sid Becker[b,2], Matej Reberšek[a,3], Damijan Miklavčič[a,4], Nataša Pavšelj[a,*]

[a] University of Ljubljana, Faculty of Electrical Engineering, Tržaška 25, SI-1000 Ljubljana, Slovenia
[b] University of Canterbury, Mechanical Engineering Department, Private Bag 4800, Christchurch 8140, New Zealand

ARTICLE INFO

Article history:
Received 27 July 2013
Received in revised form
11 September 2013
Accepted 15 September 2013
Available online 26 September 2013

Keywords:
Transdermal delivery
Electroporation
Square wave pulses
Franz diffusion cells
Numerical model

ABSTRACT

Electroporation can be used as an active enhancement method for intra- and transdermal drug delivery. Differences in response of skin to electric pulses depend on their amplitude, duration and number and have been a point of interest in the past. While protocols consisting of the same repetitive, mostly exponentially decaying pulses have been used before, this study is focused on comparing different combinations of square wave short high voltage (HV) and longer low voltage (LV) electroporation pulses. Our in vitro experimental results show that longer LV pulses significantly increase subsequent passive transport of calcein through dermatomed pig skin, while short HV pulses alone result in negligible calcein passive transdermal transport. Surprisingly, when the long LV pulses are preceded by short duration HV pulses, the total calcein transported is reduced significantly. This result is explained using a theoretical physics based model of individual local transport region (LTR) evolution during the applied LV pulse. The theoretical model shows that HV pulses alter the structure of the stratum corneum in such a way that when the LV pulses are applied, insufficient thermal energy is generated to initiate LTR expansion. Together, the experimental results and theoretical predictions show that the total pulse energy alone cannot account for total solute transport: that the order of the types of pulses administered must also be considered. Our findings open a direction for further improvement of the method using new protocols.

1. Introduction

In the past decades, the topic of intra- and transdermal drug delivery has become a field of biomedical research with rapid development. The success of this delivery route, however, depends on the ability of the drug to permeate the skin barrier in sufficient quantities to achieve its desired pharmacological effect. Modification of skin permeability to increase transdermal delivery has been achieved by passive (penetration enhancers, liposomes, nanoparticles, patch technology) and active methods of enhancement (electroporation, iontophoresis, microneedles, ultrasound, laser radiation). While passive methods are based on the formulation and chemical approaches, active employ physical force to overcome the skin barrier and/or provide a driving force on the drug (Williams, 2004; Zorec et al., 2013).

Electroporation is a well established and widely used method able to transiently create aqueous pores in phospholipid bilayers of cell membranes, using electric pulses of high voltage and short duration. It has also successfully been used to enhance skin permeability for molecules with different lipophilicity and size (small molecules, proteins, peptides and oligonucleotides), including biopharmaceuticals with molecular weight greater than 7 kDa (Denet et al., 2004; Denet and Préat, 2003). In addition, electroporation can also be used for applications where, after intradermal injection, the therapeutic molecules need to be inserted in the viable skin cells, or for gene transfection (André et al., 2008; Daugimont et al., 2010; Pavselj and Préat, 2005; Zibert et al., 2011). Transdermal transport after skin electroporation depends on the shape, amplitude, duration and the number of the electric pulses. When comparing different pulse protocols, pulse length and amplitude are the most influential factors in electroporation-based applications. Namely, to achieve the transmembrane voltage required for cell membrane permeabilization, a high enough pulse amplitude is essential. On the other hand, longer pulses are necessary to ensure higher

Abbreviations: SC, stratum corneum; LTR, local transport region; HV, high voltage; LV, low voltage.

* Corresponding author. Tel.: +386 1 4768 765; fax: +386 1 4264 658.
E-mail addresses: barbara.zorec@fe.uni-lj.si (B. Zorec), sid.becker@canterbury.ac.nz (S. Becker), matej.rebersek@fe.uni-lj.si (M. Reberšek), damijan.miklavcic@fe.uni-lj.si (D. Miklavčič), natasa.pavselj@fe.uni-lj.si (N. Pavšelj).
[1] Tel.: +386 1 4768 121.
[2] Tel.: +64 3 364 2987x7231.
[3] Tel.: +386 1 4768 121.
[4] Tel.: +386 1 4768 456.

0378-5173/$ – see front matter © 2013 Elsevier B.V. All rights reserved.
http://dx.doi.org/10.1016/j.ijpharm.2013.09.020

cumulative pulse energy, crucial for electrophoretic or resistive heating effects when needed.

It has been shown that molecular and ionic transport across the skin exposed to a number of high voltage pulses is highly localized in sites termed local transport regions (LTRs) (Pliquett, 1999; Pliquett and Gusbeth, 2004; Vanbever et al., 1999; Weaver et al., 1999). The size of the LTRs depends on cumulative pulse duration, while pulse amplitude dictates their density. The expert opinions in the field are in general agreement that there are different responses according to two primary pulsing regimes: short duration-high voltage (HV) pulses result in an altered stratum corneum (SC) that is perforated with micrometer-sized aqueous pathways while long duration low voltage (LV) pulses result in regions of increased permeability within the SC that are relatively large (up to hundreds of μm) and long lasting (Denet et al., 2004; Pliquett et al., 1996, 2005, 2008; Pliquett and Gusbeth, 2004; Vanbever et al., 1999). The structural alterations associated with the short pulse regime are accompanied by an increase in SC conductivity, which occurs within less than ~10 μs, when the voltage drop across the SC exceeds certain critical value (above ~50 V) (Denet et al., 2004; Pliquett et al., 2008; Pliquett and Gusbeth, 2004).

The response of the skin in the long low voltage (LV) pulse regime occurs at much longer timescales (up to hundreds of ms) and is associated with the development of "large" regions of altered SC. These long duration induced local transport regions (LTR) are formed in the sites of the so-called stratum corneum "defects" (Pliquett, 1999) that are expanded by resistive (Joule) heating. These large regions can originate as groupings of several of smaller pathways which expand to length scales of hundreds of μm. The large region of affected SC that results from this expansion is termed "local transport region" (LTR) because within this region the permeability is several orders of magnitude higher than in the surrounding unaltered SC. The development of the LTR is believed to be associated with resistive – Joule – heating which has been documented under certain experimental pulse conditions to cause localized temperature rises of over 60 °C (Pliquett et al., 1995, 2005, 2008; Pliquett and Gusbeth, 2000, 2004; Prausnitz, 1996; Vanbever et al., 1999).

The use of electric pulses on skin is not a new research topic. A number of studies have been performed, using both theoretical (Pavselj and Miklavcic, 2008; Pavšelj and Miklavčič, 2008, 2011) and experimental approach to explain the mechanisms involved. Since different parameters of electric pulses exert different effects on the stratum corneum, finding an optimal protocol has been a point of interest in the past. Earlier (and most) experiments were performed using repetitive exponentially decaying pulses (Pliquett et al., 1996, 2005; Pliquett and Gusbeth, 2000; Prausnitz et al., 1993; Regnier et al., 1999; Vanbever et al., 1998, 1999) of different amplitudes, durations and numbers, for two reasons: (i) the technology of capacitor-discharge devices delivering exponentially decaying pulses is much simpler than the technology behind square wave generators and (ii) the long low voltage tail of such pulses provides the electrophoretic part of the pulse, and is responsible for most of Joule heating, adding further to the success of transdermal delivery. On the other hand, to achieve better control of protocol parameters, square wave pulses are preferred (Denet et al., 2003; Denet and Préat, 2003; Dujardin et al., 2001, 2002). Again, different amplitudes, durations and number of square wave pulses have been used for transdermal delivery, albeit always with protocols composed of a number of one same type of pulses.

In our study we experiment with different combinations of square wave short high voltage (HV) and long low voltage (LV) pulses, focusing primarily on the order of pulses. The importance of the order of different types of pulses has been shown before in electroporation-based applications (Pavlin et al., 2010). However, to our knowledge, experiments that vary the sequence of different types of square wave pulses have not been done so far in studies that use electroporation to enhance transdermal delivery. The influence of pulsing protocol on calcein transdermal delivery associated with electroporation is investigated by using a combination of experimental observation and theoretical modeling. We begin with the experimental component of the study in which the total solute transported across the SC is measured for different pulse protocols in vitro. The second part is a theoretical description of the LTR development and its link to the observed experimental results, giving new insights into the mechanisms involved in skin electroporation. The authors have developed thermodynamic based models that directly relate the internal energy of the SC lipids to the degree of disorganization of the SC microstructure, linking it to molecular transport (Becker, 2011, 2012; Becker and Kuznetsov, 2007, 2008).

2. Materials and methods

2.1. In vitro experiments

2.1.1. General experimental setup

Vertical glass Franz diffusion cells were used to study molecular transport through excised and dermatomed pig skin. The temperature of the chamber was regulated at 37 °C by water circulation. A piece of porcine dermatomed skin was placed between two compartments with the stratum corneum facing the donor compartment. The area of skin available for diffusion was 0.785 cm^2. The receiver compartment (3.1 ml) was filled with PBS (pH 7.4, 150 mM), in order to maintain a constant pH and the osmolarity as well as to match ion concentration to that of human body. The donor compartment contained 1 ml of calcein solution (0.1 mM) in phosphate buffer (pH 6.5, 100 mM). For pulse delivery we used a unipolar square wave pulse generator Cliniporator (Igea, Italy). The pulses were delivered into the donor and the receiver compartment through 1 mm diameter platinum wire electrodes ending with a plate that is placed 0.2 cm away from the skin in donor compartment and 0.5 cm in the receiver compartment. As calcein is negatively charged, negative electrode was placed in donor and positive electrode in receiver compartment. When the skin is exposed to sufficiently intense electric pulses, its outer barrier, the stratum corneum undergoes a "breakdown" in its barrier properties due to local alteration of the microstructure of the stratum corneum lipids. The extent of the size of these alterations can vary by several orders of magnitude from the single pore (~10 nm) up to a larger local transport region (LTR) (~100 μm). Differences in response to electric pulses depend on pulse amplitude, duration and number. In order to study these differences, we experimented with both: short high voltage (HV) and long low voltage (LV) pulses, varying pulse number and order. Generally accepted postulation is that: (a) short, HV pulses (hundreds of μs) will result in the creation of small cell-level permeation pathways through the stratum corneum and (b) longer (hundreds of ms), low amplitude pulses will expand these pathways into the much larger LTRs, as well as provide some driving force for a charged solute before subsequent passive diffusion. The parameters of the HV pulses were: 500 V, 500 μs duration, 500 μs spacing between pulses (when applicable). Further, the parameters of LV pulses were: 45 V, 250 ms duration, 100 ms pulse spacing (when applicable). When HV pulses were followed by LV pulses, no delay between the HV and the LV part of the protocol was used. Pulse protocols and experimental conditions of the study are summarized in Table 1:

2.1.2. Chemicals and sample preparation

Calcein and sodium chloride were purchased from Sigma–Aldrich (St. Louis, MO, USA), while potassium chloride, di-sodium

Table 1
Pulse protocols and experimental conditions of the study.

	Parameters
Pulse protocols	3xHV 3xLV 1xHV + 1xLV 3xHV + 1xLV 1xHV + 3xLV 3xHV + 3xLV (HV + LV)x3 3xLV + 3xHV
HV pulses	Amplitude: 500 V Length: 500 μs Spacing: 500 μs
LV pulses	Amplitude: 45 V Length: 250 ms Spacing: 100 ms
Experimental setup	Donor: 1 ml calcein (0.1 mM) in phosphate buffer (pH 6.5, 100 mM) Receiver: 3.1 ml PBS (pH 7.4, 150 mM) Diffusion area: 0.785 cm^2 Temperature: 37 °C

hydrogen phosphate and potassium dihydrogen phosphate were purchased from Merck (Darmstadt, Germany). PBS buffer solution was prepared in bi-distilled water (8 g NaCl, 0.2 g KCl, 1.44 g Na_2HPO_4, 0.24 g KH_2PO_4 in 1 l of water), as well as phosphate buffer solution (7.38 g NaH_2PO_4, 4.77 g Na_2HPO_4 in 1 l of water). In order to mimic physiological conditions, the receiver compartment was filled with PBS (pH 7.4). After preliminary comparison of different buffers and their effectiveness in maintaining the pH during the application of long low voltage pulses, we used phosphate buffer (pH 6.5) for the donor solution. This is very important especially in the donor compartment, where the small volume of the solution makes pH shifts of the solution more marked. The change in pH can also change the charge of the molecule thus influencing its flux through the skin.

Fresh pigs' ears were obtained from slaughter house Farme Ihan d.o.o., Šentjur, Slovenia. We provided all the documentation needed for working with animal by-products in our laboratories. The skin was removed from the ears approximately 2 h post-mortem and dermatomed to 350 μm thickness (TCM 3000 BL, Nouvag®). Skin samples were stored at −21 °C until use.

2.1.3. Skin voltage measurements

As the electrodes were not in close contact with skin and the pulses were delivered into the donor and the receiver solution, only a fraction of the voltage delivered by the pulse generator was established across dermatomed skin. This U_{skin} was measured during the experiments with two thin copper wires (diameter: ∼0.3 mm) that were placed directly on the skin. One was placed right under the dermatomed skin and the other one facing the stratum corneum. The inertness of the measuring electrodes was not crucial for the experimental setup and the protocols used, therefore, we used the cheaper and readily available copper electrodes instead of platinum or Ag/AgCl. Further, to avoid leaking and electric field interference, measuring electrodes needed to be as thin as possible. Pulses were delivered through the setup described above (Section 2.1.1). Voltages (both $U_{delivered}$ and U_{skin}) and electric current were measured with LeCroy Oscilloscope (Wavepro 7300A) using differential voltage probes (ADP305, High Voltage Differential Probe, LeCroy) and current probes (AP015, LeCroy).

2.1.4. Data analysis

The concentration of calcein in receiver compartment after pulse delivery was measured using spectrofluorometer (Jasco, FP-6300). This method was used because, due to the inertness of platinum electrodes and low number of pulses used, we assumed that no electrode byproducts were created during pulse delivery. At each sampling time, a sample of 300 μl of receiver solution was taken for concentration measurement and replaced with fresh PBS. Concentration was calculated accordingly. We monitored the concentration of calcein in the receiver solution every hour for 5 h after pulse delivery. Before and after electroporation we also measured pH of donor and receiver solutions.

The results were expressed as the mean ± standard error of the mean (normality test passed in all instances). Statistical tests One way analysis of variance (One Way ANOVA) were performed on all results (SigmaStat 3.1, Systat, USA). A 0.05 level of probability was taken as a level of significance.

2.2. Theoretical work

Our thermodynamic model describes the thermo-electrical behavior in a small region of the skin sample during long LV pulses. This region surrounds an evolving LTR that originates within a very small SC defect whose radius lies in this study within the range: 2.5 μm ≤ R_P ≤ 15 μm. These cell-level pathway sizes were expected either after pulsing with the rather long (500 μs) HV pulses used in our study or as pre-existing appendage-associated pathways. Because the computations focus on a single LTR, the computational domain size is much smaller than the experimental skin sample. The outer radius of the computational domain (R_O) lies within the range: 50 μm ≤ R_O ≤ 500 μm, representing different LTR densities. Even though this means that the theoretical model could represent as little as 1/10,000 of the actual experimental skin sample, the idea is that there exists a distribution of LTRs within the actual skin sample, each of whose behavior is reflected by the results of the theoretical model.

For a detailed mathematical description of this theory, the reader is referred to reference Becker (2012). The concept of this computational model is that in the regions of the SC where the electrically-created pathways have been initiated or in the vicinity of skin appendages, the SC has a much higher effective electrical conductivity. Thus the electric field (which is evaluated from the Laplace equation) will be very non-uniform laterally along the SC. Within the localized region of higher electrical conductivity, the local electric current density may become sufficiently high to result in significant local resistive heating. The local temperature is evaluated from the heat conduction equation. At lipid phase transition temperatures around 65 °C, any increase in the local lipid internal energy will result in an aggregation of the local lipid microstructure (Cornwell et al., 1996). Theoretically then, the LTR region of influence may be linked directly to the thermal state of the SC lipids. This is done in references Becker (2011, 2012) and Becker and Kuznetsov (2007, 2008) using a square shaped enthalpy-temperature curve that directly relates the degree of the lipids' lamellar disorganization to the local internal energy. This magnitude of lipid disorder is then related directly to the coefficients: electrical conductivity, electrophoretic mobility, and diffusion coefficient. The transport is derived from the modified Nernst–Planck equation which includes transient electrophoresis and passive diffusion. Even the longest electroporation pulses are usually only tens to hundreds of ms long so that the influences of electro-osmosis are negligible compared to the electrophoretic contribution (Denet et al., 2004; Regnier et al., 1999; Satkauskas et al., 2005) and have been neglected here, as well as the contribution of passive diffusion during pulse delivery. At times between pulses, or after the application of a series of pulses (e.g. for 5 h after pulse delivery), passive diffusion is the only, and overall predominant transport mechanism.

The skin is modeled as a donor-compartment/skin/receiver-compartment composite system whose thermo-electrical property values are listed in Table 2. Dermatomed skin used in experiments

Table 2
Physical and geometrical parameters of the model.

	Solution	SC	Epidermis	Dermis
Thickness (μm)	Dnr 12940 Rcvr 39306	20	50	300
Thermal conductivity (W/mK)	0.6	0.2	0.209	0.293
Density (kg/m^3)	1000	1500	1110	1116
Heat capacity (J/kg K)	4180	3600	3600	3800
Electrical conductivity (S/m)	1	1×10^{-4} (*SC-U*) 5×10^{-2} (*SC-M*)	0.1	0.15
Electrophoretic mobility (m^2/V s)	1.5×10^{-8}	1×10^{-15} (*SC-U*) 1×10^{-10} (*SC-M*)	1×10^{-9}	1×10^{-9}
Diffusion coefficient (m^2/s)	1.5×10^{-10}	1×10^{-16} (*SC-U*) 1×10^{-16} (*SC-M*)	2×10^{-11}	2×10^{-11}

Notes: SC electrical conductivity, electrophoretic mobility, and diffusion coefficient vary depending on SC condition. Values associated with *SC-U* correspond to unaltered SC, values associated with *SC-M* correspond to those of the SC at full lipid phase transition: these are the maximum values within the LTR.

was modeled as a layered structure, consisting of the stratum corneum, the epidermis and some dermis. The described geometry was not static, as the transport pathways were dynamically expanding during pulses (LTR expansion for temperatures above 65°, see above). In this way, the model also describes changes in stratum corneum conductivity, leading to changed electric field distribution in the tissue (electrically, this layered structure is a voltage divider). Namely, these changes during pulse delivery affect both, LTR expansion due to resistive heating, as well as electrophoretic force, and need to be accounted for. We did, however, omit electrical conductivity changes of epidermal and dermal layer in the model, but since these changes are much smaller than those in the stratum corneum, the error thus introduced is small. Geometric parameters used in this model were taken as representative of porcine ear skin from reference Jacobi et al. (2007). The SC electrical conductivity values listed in Table 2 have been chosen to represent the two order of magnitude increase in electrical conductivity with lipid restructuring as suggested in Pliquett (1999). Electrical conductivity values of the epidermis and dermis were representative of values published in Miklavčič et al. (2006). Thermodynamic values shown in Table 2 are taken from previous studies that model the composite nature of the skin (Becker, 2011, 2012; Becker and Kuznetsov, 2007, 2008). The transport coefficients of calcein are conservative and have been chosen based on interpretation of published work (Zador et al., 2008). Within the SC, the transport coefficients are modeled to undergo several order of magnitude increases. This reflects the dramatic increases in permeability associated with the development of the LTR.

3. Results and discussion

3.1. Experimental data

As the pulses are delivered to skin in Franz diffusion cells via the buffered donor and receiver solution, we first examined what percentage of the delivered voltage is established across dermatomed skin during HV and during LV pulses alone. Signals recorded with oscilloscope during 3xHV and 3xLV protocols are shown in Figs. 1 and 2, respectively: upper panels denote the voltage delivered with Cliniporator into the solution (gray line), and the voltage measured across skin (black line); electric current is shown in the bottom panels. Please note very different time scales on Figs. 1 and 2: the difference in length between the long LV pulses and the short HV pulses is three orders of magnitude. The difference in amplitude, however, is only one order of magnitude. Before and after pulse delivery, pH was measured in both, the donor and the receiver solutions. For the pulse parameters used, we observed no changes in pH value.

As depicted in Figs. 1 and 2, the voltage measured across skin (U_{skin}) is slowly decreasing during pulse delivery while, at the same

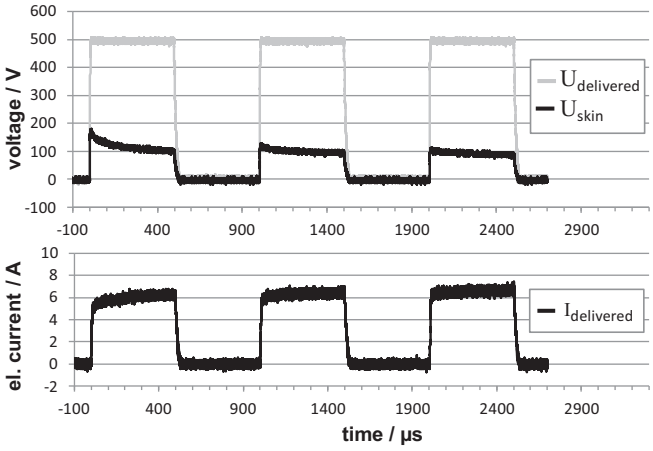

Fig. 1. Voltage and electric current during 3xHV pulse protocol. Upper panel: the voltage delivered with pulse generator (gray), voltage measured across skin (black); bottom panel: the electric current. Note very different time scales when comparing this figure to Fig. 2.

time, the electric current is increasing. This suggests an increase in overall skin conductivity. If we compare the magnitude of these changes during 3xHV protocol (Fig. 1) to the changes during 3xLV protocol (Fig. 2), we can observe higher increase in conductivity during the LV pulses.

Some of the results of the total calcein concentration in the receiver compartment for 5 h of passive diffusion after pulse delivery are shown in Fig. 3. For clarity, only some of the protocols are

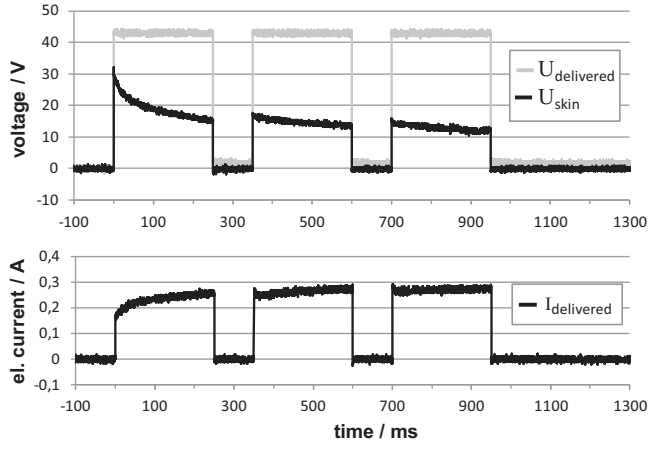

Fig. 2. Voltage and electric current during 3xLV pulse protocol. Upper panel: the voltage delivered with pulse generator (gray), voltage measured across skin (black); bottom panel: the electric current. Note very different time scales when comparing this figure to Fig. 1.

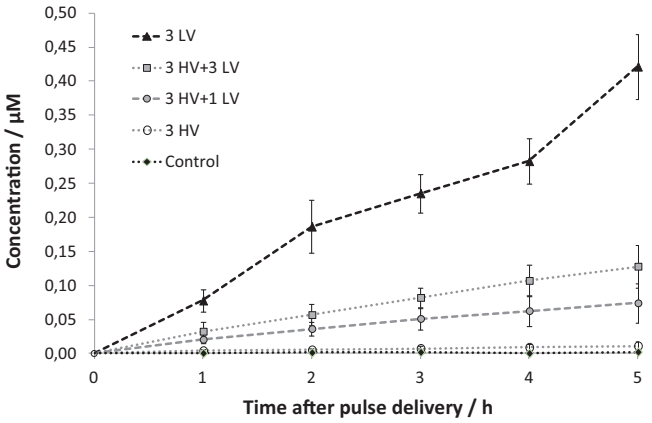

Fig. 3. Comparison of different pulse protocols and their effect on skin and subsequent passive calcein delivery through the skin. The concentration of calcein in the receiver compartment was measured for 5 h following pulse delivery (at time zero).

included. The concentrations of calcein at 5 h after pulse delivery for all pulse protocols used are given in Table 3. Firstly, the control without any applied pulses results in negligible transfer. This is expected due to the formidable barrier that SC represents for molecular transport of even relatively small molecules. Also, calcein in free solution has a small associated diffusion coefficient (Milanova et al., 2011; Stenekes et al., 2000; Zhao, 2008). Further, calcein concentration for 5 h after 3xHV protocol is very low, showing nearly negligible improvement from the case without any pulses delivered. This seems to imply that our 3xHV pulses have a negligible influence on subsequent calcein delivery by passive diffusion. Recalling that the SC structural alterations associated with the short HV pulses result only in small, cell-level pathways, this is not surprising. Consider now the striking contrast in the transport response to the low voltage pulses (3xLV protocol). Here we see a significant quantity of calcein transported through the skin by passive diffusion after the longer, low voltage pulses, with almost constant rate of transport sustained over the 5 h of testing. This is consistent with a very large increase in SC permeability that is anticipated in the creation of "large" LTRs that are associated with long LV pulses.

The differences between the skin's response to HV or LV square wave pulses has been a point of interest in the past (Denet and Préat, 2003; Dujardin et al., 2001, 2002). However, of further interest to this study is the effect that these pulsing protocols have on the skin when used in combination with one another. Thus we also compared different combinations of short high voltage (HV) pulses and longer low voltage (LV) pulses and their effects on skin to enhance passive transport of calcein through the skin. We anticipated that a combination of HV, followed by LV pulses will work in synergy and will result in more transport of the solute through skin than either HV or LV alone. The rationale behind this expectation states that (a) the short, HV pulses will result in the creation of small cell-level permeation pathways through the stratum corneum and (b) the longer (hundreds of ms), low amplitude pulses will expand these newly created pathways into the much larger LTRs, as well as provide some driving force for a charged solute before subsequent passive diffusion.

However, contrary to this expectation, we found that HV pulses have a negative effect on calcein delivery compared to LV pulses alone. The transport of calcein through the skin increases with increasing number of LV and is significantly decreased when preceded by HV pulses (see Fig. 3 and Table 3).

In order to better understand the phenomena observed when HV and LV type pulses are used in combination, we look again at the effects when the pulses are applied separately. The HV pulses alone result in an increase in electrical conductivity (as suggested by electric current increase shown in Fig. 1), but negligible increases in permeability to passive transport of calcein: this implies the expected small, cell-level pathways through the SC which are large enough for electric current, but too small for significant passive diffusion of calcein. The LV pulses alone result in increase in electrical conductivity (inferred from marked electric current increase in Fig. 2) while also resulting in long term increases in diffusion related transport of calcein: this is in line with the expansion of the LTR during the LV pulse. It has to be emphasized that calcein can be transported even through smaller, cell-level pathways, however, electrically-driven transport (sufficient electrophoresis or iontophoresis) is needed in this case. To achieve transport with mostly passive diffusion (as in our case), larger LTRs are needed. Inside these larger transport pathways, no or little recovery takes place for hours (even up to days) after pulses, as reported in the literature (Pliquett, 1999). Experimental results shown on Fig. 3 demonstrate fairly constant rate of passive transport (the slope of calcein concentration increase over time), suggesting no resealing during the 5 h of the experiment, which is in line with the reported findings on LTRs (Pliquett, 1999).

We infer from our experimental data that the small, cell-level pathways within the SC resulting from the HV pulse somehow inhibit the formation of the LTR which result from the LV pulse. This leads to the question: why or how does the existence of densely distributed small pathways prior to the application of an LV pulse interfere with the subsequent evolution of the highly permeable LTRs? The reason for the negative effect of the preceding HV pulses may be precisely the large number of cell-level pathways created with the HV pulses. Namely, the large LTRs result from localized resistive heating during the LV pulse. In order for this resistive heating to provide sufficient thermal energy to initiate SC lipid thermal phase transitions, a high current density is required. The HV induced pathways provide many locations of lowered SC electrical resistivity, so that when the LV pulse is applied, the electric current is distributed between these many pathways and cannot generate sufficient resistive heating for LTR evolution, which results in a lower transdermal delivery.

Changed electric field distribution in skin tissue as a result of high voltage pulsing has been a point of interest in the past (Pliquett et al., 2000). In their study, iontophoresis was used for hours as main mechanism of transdermal delivery after/in-between high voltage pulsing. The effects on skin of this intermittent high voltage pulsing resulted in changed electric field distribution, pertinent to subsequent electrically-driven transport by iontophoresis. Using high voltage pulsing may thus lead to a decrease in transdermal transport by iontophoresis, depending on the type and charge of molecule used, as was shown in Pliquett et al. (2000). In our study we explored another consequence of this changed electric field distribution in skin after HV pulses, which becomes evident

Table 3
Concentration of calcein in receiver compartment after 5 h of passive diffusion following pulse delivery. Mean calcein concentration and standard deviation of the mean are given for all pulse protocols.

Pulse protocol	Control	3HV	3HV + 1LV	1HV + 1LV	3HV + 3LV	1HV + 3LV	3(HV + LV)	3LV + 3HV	3LV
Mean (μM)	0.00227	0.01111	0.07404	0.08346	0.12782	0.13210	0.23279	0.27663	0.42141
St. dev. (μM)	0.00175	0.00595	0.02899	0.02047	0.03190	0.02030	0.03942	0.05652	0.04795

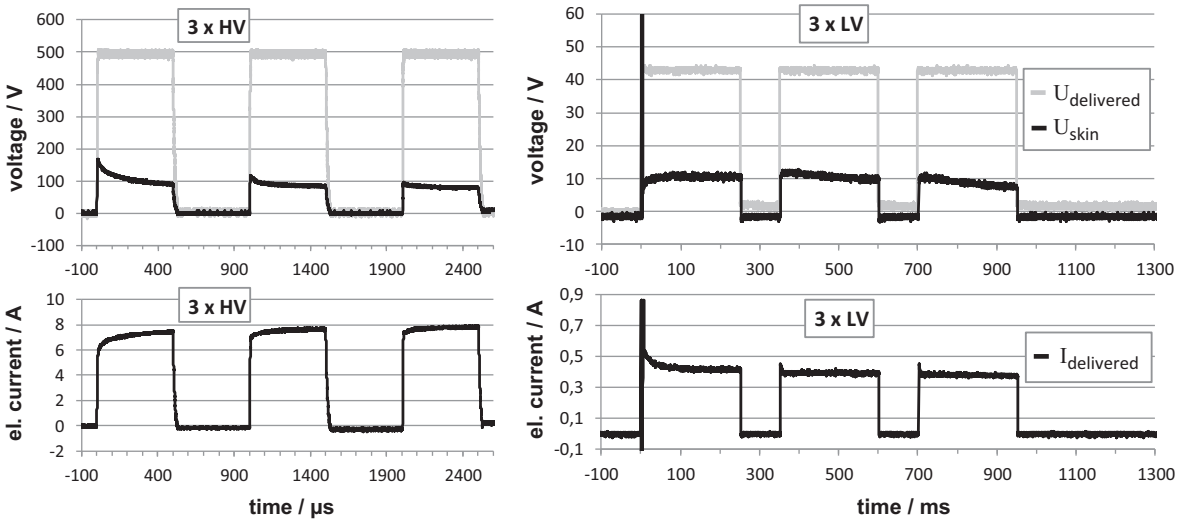

Fig. 4. Voltage and electric current during 3xHV + 3xLV pulse protocol. Upper panels: the voltage delivered with pulse generator (gray), voltage measured across skin (black) during the HV (left) and the LV pulses (right); bottom panels: the electric current during the HV (left) and the LV pulses (right). Note very different time scales between the left and the right panels: the difference in length between the long LV pulses and the short HV pulses is three orders of magnitude. What looks like a spike at the beginning of the first LV pulse (right panels) are in fact the HV pulses.

when main transport mechanism is passive diffusion: i.e. changed conditions for resistive heating and LTR expansion. This latter consequence exerts an effect directly on skin, rather than on delivered molecule, so using a different molecule would – in the case of passive transport after pulsing – yield similar results. Namely, most of the electrically-driven transport in our study occurs during the 250 ms long LV pulses, the rest is passive diffusion over 5 h of experiment. We evaluated the contributions of both transport mechanisms numerically (omitted from the manuscript due to the length constraints) and have shown, for the pulse protocols and experimental conditions used, that the electrophoretic contribution is much lower than the one from passive diffusion.

In order to examine the electrical conditions during the 3xHV + 3xLV protocol, we again recorded the voltages and the electric current during pulse delivery. Signals recorded with the oscilloscope are shown in Fig. 4. Upper panels depict the voltages delivered into the solution (gray lines), and the voltages measured across skin (black line), during the HV (upper left panel) and the LV pulses (upper right panel). Electric current is shown in the bottom panels; 3xHV: bottom left and 3xLV: bottom right. Please note very different time scales between the left and the right panels: the difference in length between the long LV pulses and the short HV pulses is three orders of magnitude. The shapes and the amplitudes of the signals during the HV pulses are, as expected, similar to those in Fig. 1, however, the electrical behavior during the following LV pulses are markedly different to that seen in Fig. 2. First, the voltage established across skin (U_{skin}) at the beginning of the first LV pulse is much lower than during 3xLV pulses alone. This indicates that the conductivity of the skin at the beginning of LV pulses is already increased; this conductivity increase is caused by preceding HV pulses, as could be expected. The most interesting signal, however, is the electric current recorded during the LV pulses following the HV pulses (bottom right panel). The electric current is higher than during the 3xLV pulses alone, which is again due to the increased skin conductivity, however, it does not increase further during the LV pulses, as it does during 3xLV pulses alone. This seems to corroborate our assumption that no significant LTR expansion occurs during LV pulses if they are preceded by HV pulses.

To further support the hypothesis that the ordering of the pulses is important, we reversed the sequence of the pulse combination, delivering 3xLV pulses first, followed by 3xHV. As expected, the delivery of the solute was significantly higher when compared to the 3xHV + 3xLV protocol (see Table 3). Also, the fact that the 3x(HV + LV) protocol yields higher transdermal delivery than 3xHV + 3xLV, seems to further support this hypothesis. However, because 3xLV protocol shows further significant increase in transport enhancement when compared to 3xLV + 3xHV, another mechanism must be involved. One of the observations we made during the experiments is the formation of air bubbles on the skin caused by LV pulses delivered into the solution, which, in combination with the HV pulses may have a sort of an occlusion effect on the transport. In regard to this, we would like to point out that two-compartment Franz diffusion cells are not the ideal in vitro setup to be used in transdermal delivery studies with electroporation as the enhancement method. Namely, the electric pulses delivered to the skin indirectly via the donor and the receiver solution bring along a number of electro-chemical effects that cannot be easily accounted for or controlled.

The following section will provide insight into the physics underlying the response of the skin to HV and LV electric pulses with a numerical model that links structural alterations of the SC to increased mass permeability and electrical conductivity, and this in turn to the (mainly) passive transport of the solute. It will further substantiate the interpretation of the experimental results in which it is inferred that LV pulses result in the evolution of the LTR and that HV pulses create a condition that interferes with the ability of LV pulses to create the LTR.

3.2. Theoretical explanation of experimental results

The following discussion is intended as an exploration of the physics underlying the response of the skin to square wave short HV and long LV pulses (presented in Section 3.1), and should not be interpreted from the perspective that the model is attempting to precisely replicate the exact experimental conditions and results.

The region of skin modeled corresponds to the development and subsequent mass transport through a single LTR. The computational domain has an outer radius of R_O. This region is radially centered about some small region of size R_P within the SC whose electrical conductivity and mass permeability are orders of magnitude higher than that of the surrounding SC. This highly conductive region is used to represent the presence of an appendageal duct (for

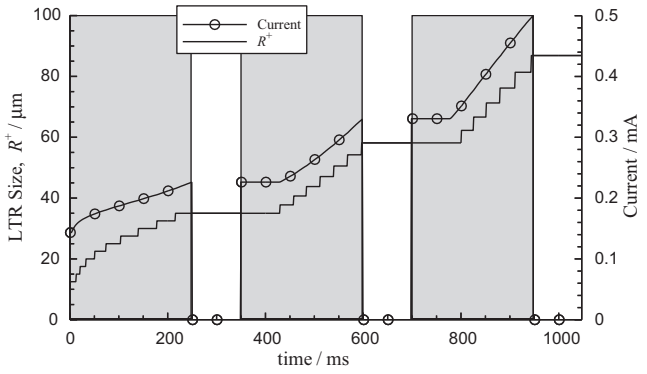

Fig. 5. Theoretical predictions of skin behavior during the LV pulses. Values shown are associated with a single LTR (initial radius 10 μm) and represent a physical domain with a lateral area that is 1/400 that of the experiment (R_O = 250 μm). Shaded regions correspond to simulated LV pulses.

large R_P), or the alteration of the SC resulting from the HV pulse (for small R_P). The theoretical predictions and discussion describes how the condition of the SC prior to the application of the LV pulse influences the development of the LTR and the associated passive transport of calcein.

In order to quantify the LTR development during the pulse, the effective LTR radius, R^+, is introduced. The effective LTR radius is defined as the minimum radial location within the SC at which the SC lipids have not experienced any thermal restructuring. This means that increases in R^+ represent the growth of the LTR's region of influence during the applied pulse.

We begin the theoretical description with a discussion of the theoretical relationship between LTR growth and electrical current increases during the application of an LV pulse train. In this scenario the outer domain radius is R_O = 250 μm and the pre-LV pulse defect radius is R_P = 10 μm. These geometries are conservative representations of size and distribution density of hairs that are found in normal porcine ear skin (Jacobi et al., 2007).

Fig. 5 presents the transient behavior of the LTR growth and the electric current during the applied LV pulses. Note that the increases in electric current reflect the LTR growth. As the LTR develops, the local electrical conductivity within the LTR increases, so that the electric current between electrodes increases as well. This provides a major point of importance in how we can interpret the electrical behavior of the experimental results. Theoretically, the increases in electric current are directly proportional to the growth of the LTR. With this in mind, consider again the experimental 3xLV electric current measurements of Fig. 2. If the transient increase of electric current during LV pulses is representative of the LTR growth/expansion as indicated by Fig. 5, then we can infer that the increases in the LV experimental current measurements shown in Fig. 2 imply LTR expansion. From this we can conclude that the constant electric current measured during the LV pulses when preceded by HV pulses (Fig. 4) does not indicate subsequent LTR expansion, which is in line with the observed calcein concentration results.

This computational domain (R_O = 250 μm) has 1/400th the lateral surface area of the experiment. Thus the theoretical model predicts a 0.14 A increase in current for the skin sample used in the experiment. Fig. 2 shows an increase in current of ~0.1 A which, while not agreeing fully, is comparable to that of the numerical model. While this is encouraging, it is also apparent that the theoretical model does not exactly capture the physics involved in experiment. This can be seen in the deviation of the model's transient electric current prediction of Fig. 5 compared to the experimental behavior of Fig. 2. The drastic increase in current of the experimental 3xLV protocol during the first pulse with little or no change in current during pulses 2 and 3 is indicative of a large alteration in global electrical conductivity of the sample during pulse 1 which is greatly reduced during pulse 2 and 3. This discrepancy is due to the simplification in our model that only captures the alterations of the SC and that neglects the conductivity changes of the rest of the skin (apart from SC).

The central question of this study was motivated by the experimental results presented in Fig. 3 and Table 3 that seem to imply that when LV pulses are preceded by even a single HV pulse, the total solute transported by subsequent passive diffusion is dramatically reduced. In the following analysis we will answer: "why does the application of HV pulses *prior* to the application of an LV pulse interfere with the evolution of the highly permeable LTRs?" In order to understand the physics underlying the reduction in total passive calcein delivery, we turn the discussion to two important points of empirical observation involving the response of the SC to HV and LV pulses (Denet et al., 2004).

(1) When the pulse intensity is decreased and the pulsing time is increased, the resulting transport regions are more likely to cluster together in groups. This is to say that the HV pulses will result in smaller areas of SC alteration (smaller R_P).
(2) When pulse amplitude is increased, the density distribution of pathways is higher. This is to say that HV electroporation pulses result in more cell-level pathways per cm^2 occurring across the lateral surface of the SC (smaller R_O).

The alteration of the SC by the HV pulse is represented in this study by the condition of the SC prior to the LV pulse.

Consider point (1) first: that the application of the HV pulse(s) results in defect formations that occupy very small regions of the SC. In the following discussion, these defects are represented theoretically by a pre-existing pathway of radius R_P (Here the term pre-existing refers to prior to the LV pulse application). The goal is to see what effect the pre-existing pathway size has on the evolution of the LTR.

The alteration of the SC by the HV pulse(s) is represented by a pre-existing (to the LV pulse) region within the SC, whose thermo-electrical properties are modeled to be the same as the donor solution. In Fig. 6a it is evident that the LTR growth is strongly dependent on the initial state of the SC. In fact is appears that there exists a lower limit of pre-existing pathway size for which substantial LTR growth can be initiated. This is evident in the R_P = 2.5 μm case for which the LTR reaches a maximum size and does not develop further over the duration of the applied pulse. This seems to imply that there is a critical value of pre-existing pathway radius that will result in sufficient Joule heating for lipid melting. The pre-existing pathway size strongly influences the distribution of electric field which in turn influences the amount of the Joule heat and thus local temperature rises. Within the pathway, the magnitude of the current density determines the magnitude of the Joule heat which in turn induces LTR growth.

The theoretical implications of Fig. 6a are that if the HV-created pathways are clustered together in localized regions of very small effective diameter (this is expected for an HV pulse), the LV pulse cannot deliver sufficient power to induce lipid phase transition which is a requisite for large LTR formation and subsequent passive mass transport.

Next we consider the second point of the empirical observations: that HV electroporation pulses result in more pathways per cm^2 occurring across the lateral surface of the SC. To investigate the effect that a higher global distribution density of pathways across the SC has on the evolution of the LTR during the LV pulse, we consider varying the radial size of the computational domain, R_O. Pathway density is inversely proportional to the square of the outer

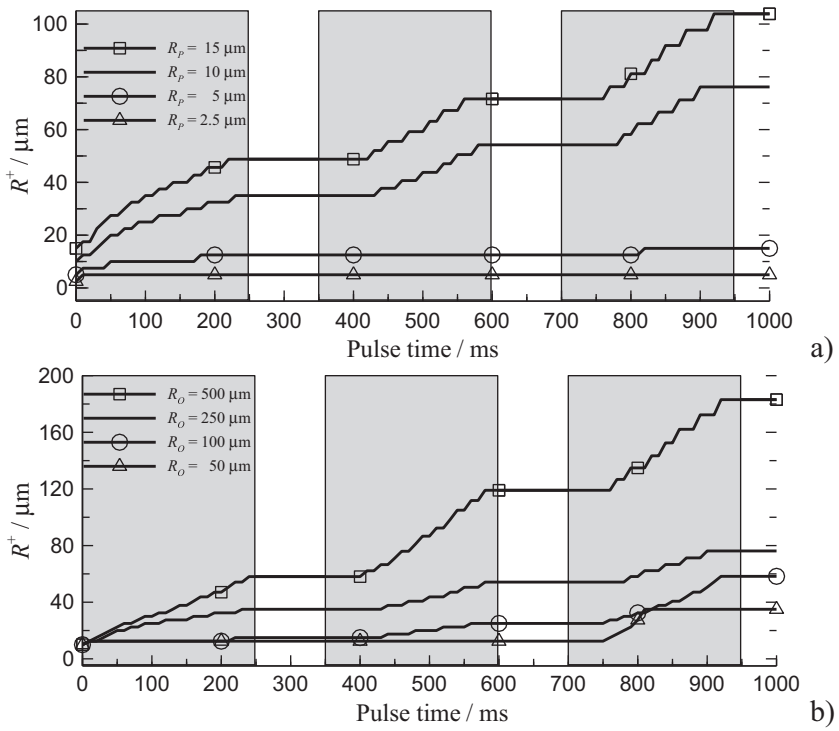

Fig. 6. (a) Theoretical influence of pre-existing defect size (R_P) on the LTR evolution size (R^+); (b) Theoretical influence of pathway density on the LTR evolution. Pathway density is inversely proportional to the square of the outer domain radius, R_O^2. Shaded regions correspond to simulated LV pulses.

domain radius, R_O^2, so that a larger value of R_O is representative of a lower distribution density of pathways.

Fig. 6b shows that the LTR evolution during the LV pulse is strongly affected by the density distribution. In fact it suggests that for a given skin sample, there is some minimum value of R_O (corresponding to maximum pathway density) below which LTR evolution does not take place. This is again in agreement with the experimental results of Fig. 3.

The physical explanation of this phenomenon lies in the consideration of the electric field. Recall that the resistive heating which is responsible for the LTR initiation results from the high current density in the small pre-existing defect region. When the pathway density is increased, the global distribution of electric current is distributed among more pre-existing pathways: effectively the total current is divided by the number of pathways. A higher density distribution of defects results in a lower electric current within each defect. The calculations used to arrive at Fig. 6b use smaller computational domain sizes to represent higher pathway densities: so that there is less total current available for a smaller R_O (representing the higher density distribution of pathways, associated with HV pulses).

We conclude this discussion with an analysis of transport that focuses on the pre-LV pulse condition of the SC. Here we compare the calcein passive delivery associated with two different scenarios of SC condition. The first scenario reflects the SC whose lateral surface is perforated with a high density distribution of very small pathways. The outer domain radius is $R_O = 100\,\mu m$ with a pre-existing pathway radius of $R_P = 2.5\,\mu m$. This is representative of the condition of the SC following 3xHV pulses. The second scenario describes the SC in the absence of HV pulses. In this case, the skin is perforated by moderately large appendage-associated pathways ($R_P = 10\,\mu m$) that are much more sparsely distributed ($R_O = 100\,\mu m$). Beginning with these SC conditions, we consider the subsequent LTR evolution during the applied LV pulses and then calculate the total solute transported with passive diffusion through the skin sample for up to 5 h after the application of the LV pulses. In order to quantify the calcein transported we use the average receiver calcein concentration: C_R. This is defined as the ratio of total calcein transported into the receiver cell to the total volume of the receiver cell and may be directly compared to the experimentally observed calcein concentrations of Fig. 3. The theoretical receiver concentrations after electroporation are plotted in Fig. 7. These show that the pre-LV condition of the SC strongly influences

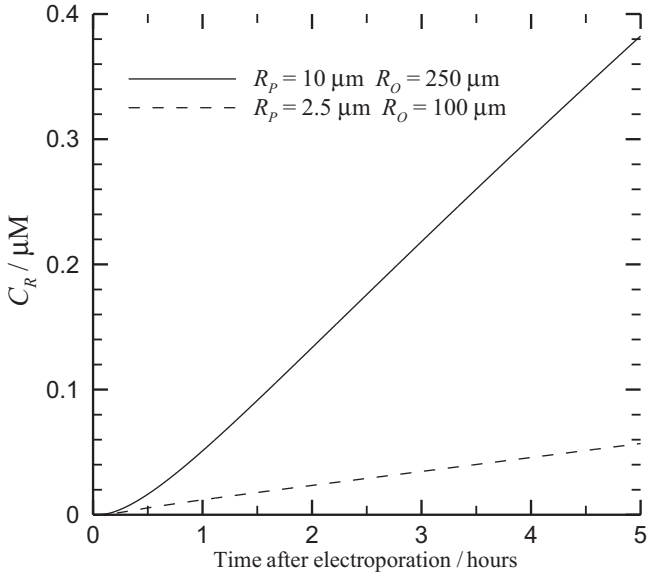

Fig. 7. Theoretical comparison of the calcein delivered through the dermatomed skin at long post pulse diffusion times. The high density small pathway case ($R_O = 100\,\mu m$, $R_P = 2.5\,\mu m$) represents the 3xHV + 3xLV pulse protocol. The low density large pathway case ($R_O = 250\,\mu m$, $R_P = 10\,\mu m$) represents the 3xLV pulse protocol.

the effect of the LV pulses on LTR formation. Here we see that the case corresponding to the condition of the SC resulting from the 3xHV pulses, followed by 3xLV pulses results in calcein concentration much lower than that of the 3xLV pulses alone. This agrees with the trends observed in experiment. It should be noted that the lateral surface of the experiment is 0.75 cm^2 and the theoretical model captures transport about a single LTR. This means that the transport for the high density distribution case (R_O = 100 μm) represents the transport through 2500 LTRs and the transport of the low density distribution case (R_O = 250 μm) represents the transport through 400 LTRs.

The total calcein transported, the electrical behavior reflected in the LTR development, and the understanding of the effects of HV pulses on the SC all provide supporting evidence that administering HV pulses prior to the LV pulses reduces the total calcein delivered through dermatomed skin. This is primarily due to the strong influence that the structural alterations associated with the HV pulses have on the electro-thermal behavior of the SC during subsequent LV pulses. Any effect that introduces more pathways of lowered electrical resistance into the SC will result in lowered LTR evolution and thus in less total calcein transport during subsequent passive diffusion.

4. Conclusions

We experimented with different combinations of square wave short high voltage (HV) and long low voltage (LV) pulses, focusing primarily on the order of pulses. Although a number of studies comparing different pulse protocols for transdermal delivery have been done in the past, the topic of pulse order have not been explored so far. It has been shown experimentally that high voltage (HV) pulses result in smaller but denser high conductivity pathways across SC, while the evolution of larger local transport regions (LTRs) during longer low voltage (LV) pulses has been shown to be a thermal phenomenon due to resistive heating and phase transition of SC lipids. Contrary to intuitive expectation – that a combination of HV pulses, followed by LV pulses will work in synergy – our results show that higher increase in skin permeability and subsequent passive transdermal delivery can be achieved with LV pulses alone. Even more, preceding HV pulses seem to have a negative effect on calcein delivery.

We supplement the measurements of calcein delivery through dermatomed skin with recordings of voltages and electric current during pulse delivery and a thermodynamically based theoretical description of the physics underlying the development of LTRs. We conclude that any influence that acts to increase the density distribution of SC regions of higher electrical conductivity or/and acts to decrease the size of these regions of higher electrical conductivity will result in the evolution of smaller LTRs. Because the application of the short HV pulses has been shown to encourage both of these and because the LTRs are associated with a higher permeability to mass transport, we explained, theoretically, why delivery is inhibited when LV pulses are preceded by HV pulses. We have thus shown that the total pulse energy (depending on pulse amplitude and duration) alone cannot account for total solute transport and that the order of the types of pulses administered must also be considered when skin electroporation is used to increase transdermal delivery. To put it simply: electric field distribution, which dictates conditions for resistive heating and LTR expansion during LV pulses is altered by preceding HV pulses.

Most experiments performed on skin electroporation for transdermal delivery so far were using exponentially decaying pulses of different amplitudes, durations and numbers. Both high voltage and low voltage pulse protocols are reported, however, we would like to stress that, in the case of exponentially decaying pulses, these labels have to be understood with reservations and cannot be directly compared to HV and LV labels we use when describing square wave pulse protocols. Namely, an exponentially decaying pulse inherently comprises a short but higher voltage component at the beginning, followed by the long lower amplitude decay of the delivered voltage. Effectively, this means that most studies done so far in fact employ either an approximation of different repetitive HV + LV protocols (repetitive exponentially decaying pulse protocols) or true square wave repetitive pulses of either HV or LV configuration.

Furthermore, not only pulse protocols, but also the experimental setup plays an important role in treatment outcome and the interpretation of the results. Because a significant voltage drop occurs in the solution when using in vitro diffusion cell experimental model for electroporation studies, the transdermal voltage cannot be directly controlled. For this reason, and to avoid a number of electro-chemical effects that cannot be easily accounted for or controlled, as well as to get closer to in vivo conditions, our experiments will be repeated and continued on a different experimental model.

In conclusion, although considerable effort has been put in the optimization of pulse protocols for transdermal drug delivery with electroporation, our study shows that the possibilities for further improvement of the method using new protocols are far from being exhausted. Also, the use of theoretical support for explanation of experimental results is crucial as it offers new insights into the underlying mechanisms and allows for better planning of future experiments. For easier and better comparison of different experimental protocols and to achieve better control of protocol parameters, the use of square wave pulses instead of exponentially decaying pulse shape is preferred.

Acknowledgments

Research was performed in the scope of LEA EBAM and was in part financed by the European Regional Development Fund (Biomedical Engineering Competence Center, Slovenia), the Slovenian Research Agency (L2-2044), and the Alexander von Humboldt Foundation. The research is a result of networking efforts of the COST TD1104 action (www.electroporation.net).

References

André, F.M., Gehl, J., Sersa, G., Préat, V., Hojman, P., Eriksen, J., Golzio, M., Cemazar, M., Pavselj, N., Rols, M-P., Miklavcic, D., Neumann, E., Teissié, J., Mir, L.M., 2008. Efficiency of high- and low-voltage pulse combinations for gene electrotransfer in muscle, liver, tumor, and skin. Hum. Gene Ther. 19, 1261–1271.

Becker, S.M., Kuznetsov, A.V., 2007. Local temperature rises influence in vivo electroporation pore development: a numerical stratum corneum lipid phase transition model. J. Biomech. Eng. 129, 712–721.

Becker, S.M., 2011. Skin electroporation with passive transdermal transport theory: a review and a suggestion for future numerical model development. J. Heat Transfer 133, 011011.

Becker, S.M., Kuznetsov, A.V., 2008. Thermal in vivo skin electroporation pore development and charged macromolecule transdermal delivery: a numerical study of the influence of chemically enhanced lower lipid phase transition temperatures. Int. J. Heat Mass Transfer, 2060–2074.

Becker, S., 2012. Transport modeling of skin electroporation and the thermal behavior of the stratum corneum. Int. J. Therm. Sci. 54, 48–61.

Cornwell, P.A., Barry, B.W., Bouwstra, J.A., Gooris, G.S., 1996. Modes of action of terpene penetration enhancers in human skin; differential scanning calorimetry, small-angle X-ray diffraction and enhancer uptake studies. Int. J. Pharm. 127, 9–26.

Daugimont, L., Baron, N., Vandermeulen, G., Pavselj, N., Miklavcic, D., Jullien, M.-C., Cabodevila, G., Mir, L.M., Préat, V., 2010. Hollow microneedle arrays for intradermal drug delivery and DNA electroporation. J. Membr. Biol. 236, 117–125.

Denet, A.-R., Préat, V., 2003. Transdermal delivery of timolol by electroporation through human skin. J. Control. Release 88, 253–262.

Denet, A.-R., Ucakar, B., Préat, V., 2003. Transdermal delivery of timolol and atenolol using electroporation and iontophoresis in combination: a mechanistic approach. Pharm. Res. 20, 1946–1951.

Denet, A.-R., Vanbever, R., Préat, V., 2004. Skin electroporation for transdermal and topical delivery. Adv. Drug Deliv. Rev. 56, 659–674.

Dujardin, N., Van Der Smissen, P., Préat, V., 2001. Topical gene transfer into rat skin using electroporation. Pharm. Res. 1, 61–66.

Dujardin, N., Staes, E., Kalia, Y., Clarys, P., Guy, R., Préat, V., 2002. In vivo assessment of skin electroporation using square wave pulses. J. Control. Release 79, 219–227.
Jacobi, U., Kaiser, M., Toll, R., Mangelsdorf, S., Audring, H., Otberg, N., Sterry, W., Lademann, J., 2007. Porcine ear skin: an in vitro model for human skin. Skin Res. Technol. 13, 19–24.
Miklavčič, D., Pavšelj, N., Hart, F.X.,2006. Electric Properties of Tissues. In: Wiley Encyclopedia of Biomedical Engineering. John Wiley & Sons, Inc., http://onlinelibrary.wiley.com/doi/10.1002/9780471740360.ebs0403/abstract
Milanova, D., Chambers, R.D., Bahga, S.S., Santiago, J.G., 2011. Electrophoretic mobility measurements of fluorescent dyes using on-chip capillary electrophoresis. Electrophoresis 32, 3286–3294.
Pavlin, M., Flisar, K., Kanduser, M., 2010. The role of electrophoresis in gene electrotransfer. J. Membr. Biol. 236, 75–79.
Pavselj, N., Préat, V., 2005. DNA electrotransfer into the skin using a combination of one high- and one low-voltage pulse. J. Control. Release 106, 407–415.
Pavselj, N., Miklavcic, D., 2008. A numerical model of permeabilized skin with local transport regions. IEEE Trans. Biomed. Eng. 55, 1927–1930.
Pavšelj, N., Miklavčič, D., 2008. Numerical modeling in electroporation-based biomedical applications. Radiol. Oncol. 42, 159–168.
Pavšelj, N., Miklavčič, D., 2011. Resistive heating and electropermeabilization of skin tissue during in vivo electroporation: a coupled nonlinear finite element model. Int. J. Heat Mass Transfer 54, 2294–2302.
Pliquett, 1999. Mechanistic studies of molecular transdermal transport due to skin electroporation. Adv. Drug Deliv. Rev. 35, 41–60.
Pliquett, U.F., Gusbeth, C.A., 2000. Perturbation of human skin due to application of high voltage. Bioelectrochemistry 51, 41–51.
Pliquett, U.F., Gusbeth, C.A., Weaver, J.C., 2000. Non-linearity of molecular transport through human skin due to electric stimulus. J. Control. Release 68, 373–386.
Pliquett, U.F., Zewert, T.E., Chen, T., Langer, R., Weaver, J.C., 1996. Imaging of fluorescent molecule and small ion transport through human stratum corneum during high voltage pulsing: localized transport regions are involved. Biophys. Chem. 58, 185–204.
Pliquett, U., Gallo, S., Hui, S.W., Gusbeth, C., Neumann, E., 2005. Local and transient structural changes in stratum corneum at high electric fields: contribution of Joule heating. Bioelectrochemistry 67, 37–46.
Pliquett, U., Gusbeth, C., 2004. Surface area involved in transdermal transport of charged species due to skin electroporation. Bioelectrochemistry 65, 27–32.
Pliquett, U., Langer, R., Weaver, J.C., 1995. Changes in the passive electrical properties of human stratum corneum due to electroporation. Biochim. Biophys. Acta 1239, 111–121.
Pliquett, U., Gusbeth, C., Nuccitelli, R., 2008. A propagating heat wave model of skin electroporation. J. Theor. Biol. 251, 195–201.
Prausnitz, M.R., Lau, B.S., Milano, C.D., Conner, S., Langer, R., Weaver, J.C., 1993. A quantitative study of electroporation showing a plateau in net molecular transport. Biophys. J. 65, 414–422.
Prausnitz, M.R., 1996. Do high-voltage pulses cause changes in skin structure? J. Control. Release 40, 321–326.
Regnier, V., De Morre, N., Jadoul, A., Préat, V., 1999. Mechanisms of a phosphorothioate oligonucleotide delivery by skin electroporation. Int. J. Pharm. 184, 147–156.
Satkauskas, S., André, F., Bureau, M.F., Scherman, D., Miklavcic, D., Mir, L.M., 2005. Electrophoretic component of electric pulses determines the efficacy of in vivo DNA electrotransfer. Hum. Gene Ther. 16, 1194–1201.
Stenekes, R.J.H., Loebis, A.E., Fernandes, C.M., Crommelin, D.J.A., Hennink, W.E., 2000. Controlled release of liposomes from biodegradable dextran microspheres: a novel delivery concept. Pharm. Res. 17, 664–669.
Vanbever, R., Leroy, M.A., Préat, V., 1998. Transdermal permeation of neutral molecules by skin electroporation. J. Control. Release 54, 243–250.
Vanbever, R., Pliquett, U.F., Préat, V., Weaver, J.C., 1999. Comparison of the effects of short, high-voltage and long, medium-voltage pulses on skin electrical and transport properties. J. Control. Release 60, 35–47.
Weaver, J.C., Vaughan, T.E., Chizmadzhev, Y., 1999. Theory of electrical creation of aqueous pathways across skin transport barriers. Adv. Drug Deliv. Rev. 35, 21–39.
Williams, A.C., 2004. Transdermal and Topical Drug Delivery: From Theory to Clinical Practice, 1st ed. Pharmaceutical Press, pp. 242.
Zador, Z., Magzoub, M., Jin, S., Manley, G.T., Papadopoulos, M.C., Verkman, A.S., 2008. Microfiberoptic fluorescence photobleaching reveals size-dependent macromolecule diffusion in extracellular space deep in brain. FASEB J. 22, 870–879.
Zhao, J., 2008. Sol–Gel Immobilized Liposomes as an Artificial-Cell-Based Biosensor for Listeriolysin O Detection. Purdue Universitiy (Doctoral dissertation) http://gradworks.umi.com/32/91/3291161.html
Zibert, J.R., Wallbrecht, K., Schön, M., Mir, L.M., Jacobsen, G.K., Trochon-Joseph, V., Bouquet, C., Villadsen, L.S., Cadossi, R., Skov, L., Schön, M.P., 2011. Halting angiogenesis by non-viral somatic gene therapy alleviates psoriasis and murine psoriasiform skin lesions. J. Clin. Invest. 121, 410–421.
Zorec, B., Préat, V., Miklavčič, D., Pavšelj, N., 2013. Active enhancement methods for intra- and transdermal drug delivery: a review. Slovenian Medical Journal, 82, http://ojs.szd.si/index.php/vestnik/article/view/1889